Published in final edited form as:
J Biol Chem. 2004 October 1; 279(40): 42139–42146. doi:10.1074/jbc.M407694200.

The Crystal Structure of *Escherichia coli* MoaB Suggests a Probable Role in Molybdenum Cofactor Synthesis*

Ruslan Sanishvili[‡,§], **Steven Beasley**[¶], **Tania Skarina**[¶], **David Glesne**[‖], **Andrzej Joachimiak**[‡,**], **Aled Edwards**[¶,‡‡], and **Alexei Savchenko**[¶]

[‡]Biosciences, Structural Biology Center, Midwest Center for Sructural Genomics, Argonne National Laboratory, Argonne, Illinois 60439

[¶]Clinical Genomics Centre/Proteomics, University Health Network, Toronto, Ontario M5G 1L7, Canada

[‖]Energy Systems Division, Argonne National Laboratory, Argonne, Illinois 60439

[‡‡]Banting and Best Department of Medical Research, University of Toronto, Toronto, Ontario M5G, Canada

Abstract

The crystal structure of *Escherichia coli* MoaB was determined by multiwavelength anomalous diffraction phasing and refined at 1.6-Å resolution. The molecule displayed a modified Rossman fold. MoaB is assembled into a hexamer composed of two trimers. The monomers have high structural similarity with two proteins, MogA and MoeA, from the molybdenum cofactor synthesis pathway in *E. coli*, as well as with domains of mammalian gephyrin and plant Cnx1, which are also involved in molybdopterin synthesis. Structural comparison between these proteins and the amino acid conservation patterns revealed a putative active site in MoaB. The structural analysis of this site allowed to advance several hypothesis that can be tested in further studies.

Molybdoenzymes are ubiquitous mediators of many essential redox reactions (1, 2). All molybdoenzymes except nitrogenase contain a molybdenum cofactor (Moco)[1] that consists of a mononuclear molybdenum covalently coordinated by molybdopterin (3, 4). In eubacteria, Moco is often modified by various nucleotides. In *Escherichia coli*, some of the molybdoenzymes contain a modified form of Moco known as molybdopterin guanine dinucleotide (MGD) (5). In some others, the metal ion is often coordinated by two MGDs (6, 7).

The biosynthesis of MGD (see Fig. 1) is catalyzed by the products of the *moa, mob*, and *moe* operons, as well as the product of the *mogA* (8) and *mobA* (9–11) genes. In eukaryotes, the homologs of MogA and MoeA are fused to form a single multifunctional multidomain protein (12), called gephyrin in mammals (13), cinnamon in *Drosophila melanogaster* (14), and Cnx1 in *Arabidopsis thaliana* (15).

*The costs of publication of this article were defrayed in part by the payment of page charges. This article must therefore be hereby marked "*advertisement*" in accordance with 18 U.S.C. Section 1734 solely to indicate this fact.
The atomic coordinates and structure factors (code 1MKZ) have been deposited in the Protein Data Bank, Research Collaboratory for Structural Bioinformatics, Rutgers University, New Brunswick, NJ (http://www.rcsb.org/).

** To whom correspondence should be addressed. Tel.: 630-252-3926; Fax: 630-252-6126; andrzejj@anl.gov..
§Present address: General Medicine and Cancer Institute Collaborative Access Team (GM/CA CAT), Argonne National Laboratory.

[1]The abbreviations used are: Moco, molybdenum cofactor; GTP, guanosine triphosphate; GDP, guanosine diphosphate; MGD, molybdopterin guanine dinucleotide; MES, 4-morpholineethanesulfonic acid.

Mutants in the *E. coli* MGD biosynthetic pathway are viable under experimental conditions, albeit with compromised phenotypes (16, 17). In humans, mutations in the enzymes of Moco biosynthesis result in a Moco deficiency, leading to several neurological complications and subsequent death at a young age (18).

The structures of members of the *E. coli* Moco biosynthesis pathway, MoaC (17), MogA (19), MobA (10, 11), MobB (20), ModE (13), MoeA (21, 22), and molybdopterin synthase ($MoaD_2$-$MoaE_2$) (23), have been determined to clarify their roles in the pathway (Fig. 1). However, the exact enzymatic activities of these proteins are not well understood. Similarly, very little is known about the biochemical and physiological roles of the MoaB protein, although it is believed that MoaB may be involved in the synthesis of precursor Z (8). BLAST data base (24) searches also indicate the involvement of MoaB in the biosynthesis of Moco. Here we report the crystal structure of *E. coli* MoaB at a 1.6-Å resolution. Amino acid sequence and structural similarities with other members of the Moco pathway strengthen the possibility of a role for MoaB.

EXPERIMENTAL PROCEDURES

Cloning and Protein Purification

E. coli MoaB was cloned, expressed, and purified using standard procedures (25). The hexahistidine tag was removed before crystallization. The purified MoaB protein was dialyzed against 10 mM HEPES, pH 7.5, 500 mM NaCl, and concentrated using a BioMax concentrator (Millipore). Before crystallization, any particulate matter was removed from the sample by passage through a 0.2-μm Ultrafree-MC centrifugal filtration device (Millipore).

Crystallization and X-ray Data Collection

Two microliters of the dialyzed MoaB protein were mixed with an equal volume of precipitant containing 2.0 M ammonium sulfate and 20% (v/v) ethylene glycol. Droplets were equilibrated against the precipitant with hanging drop vapor diffusion, and crystals grew after 2–5 days at 21 °C. For diffraction studies, the crystals were flash-frozen in liquid nitrogen with 25% (v/v) ethylene glycol added to the crystallization buffer as the cryoprotectant. The crystals belonged to the hexagonal space group P321, with the cell parameters at 100 K being $a = b = 69.11$Å, $c = 126.22$Å, $\alpha = \beta = 90°$, $\gamma = 120°$, and contained two molecules of protein/asymmetric unit. The Matthews coefficient (26) was 2.33, which corresponds to the solvent content of ~46% in crystals.

A two-wavelength anomalous dispersion experiment with crystals of Se-Met-derivatized protein was carried out on the 19ID beamline of the Structural Biology Center Collaborative Access Team of the Advanced Photon Source (Argonne National Laboratory, Argonne, IL). The absorption peak and the rising inflection point were determined by calculating and plotting f′ and f″ values against energy (27) from the fluorescence spectrum measured for a test crystal. Later, higher resolution data were collected from the unexposed part of the same crystal, which had been stored in liquid nitrogen. All crystallographic data were measured with the custom built 3 × 3 tiled charge-coupled device detector (28) with a 210 × 210-mm^2 active area and fast duty cycle (~1.7 s). The experiment, data collection, and visualization were controlled with d*TREK (29), and all data were integrated and scaled with the program package HKL2000 (30). Some of the basic statistics of data collection and processing are provided in Table I.

Guanosine Triphosphate Binding

Purified recombinant MoaB protein was subjected to binding assays using reaction conditions consisting of 0.7 mg/ml protein, 50 mM KCl, 100 nCi [α-^{32}P]GTP (3000 Ci/mmol; PerkinElmer Life Sciences), and 50 mM pH buffer (sodium acetate, pH 5.0, MES, pH 6.5, Tris, pH 7.5, Tris, pH 8.0) in a 50-μl reaction volume. Divalent cations were added as $MgCl_2$, $CaCl_2$, or $MnCl_2$ to a concentration of 5 mM. After 15 min at 30 °C, reactions were stopped, and the protein was precipitated by the addition of an equal volume of saturated ammonium sulfate in binding buffer and incubation on ice for 15 min. Pellets were collected by centrifugation, washed twice with saturated ammonium sulfate, and dried. The protein was then resuspended in 10 μl of binding buffer, and the precipitated GTP was monitored by scintillation counting using total input radioactivity as a standard.

Determination of the GTPase activity was essentially as previously described (31). Briefly, pelleted proteins were resuspended in binding buffer and hydrolyzed by adding perchloric acid to 6% concentration for 15 min. The pH was adjusted to 3.5 with potassium phosphate, the reactions were clarified by centrifugation, and aliquots were spotted on polyethyleneimine-cellulose TLC plates (Selecto Scientific Inc.). A GDP standard was enzymatically derived by the incubation of [α-^{32}P]GTP substrate with thermosensitive alkaline phosphatase (Invitrogen) in the manufacturer's supplied reaction buffer. Separation of phosphorylated reaction products was achieved by TLC using 0.65 M KH_2PO_4 as running buffer. Plates were dried and exposed to Fuji RX film.

RESULTS

Structure Solution and Refinement

Initially, only two Se sites, one from each of the molecules in the asymmetric unit, were found with the CNS (32) program, and phases were calculated to a 2.5-Å resolution. An inspection of the log-likelihood gradient maps revealed the non-isotropic nature of these sites. After phase refinement and accounting for this anisotropy, two other Se sites were also located. However, they were disordered to the extent that the phases did not improve significantly (Table II). Experimental phases were extended from 2.5- to 2.0-Å resolution with density modification, using data collected at the inflection point of the absorption edge.

The initial model for the most of both molecules was built with the program ARP/wARP (33). The remainder of the model was built and all side chains were corrected manually. This model was then refined against the 1.6-Å resolution data with several macrocycles of CNS and subsequently with REFMAC5 (34). Inspections and corrections of the model were made with the programs O (35) and QUANTA (Accelrys, Inc.).

Phasing and refinement parameters are shown in Table II. The structural coordinates have been deposited in the Protein Data Bank (36) with the access code 1MKZ.

Spatial Model of MoaB

The current model of MoaB consists of two crystallographically independent molecules, A and B. Molecule A contains 170 amino acid residues and has Met^1 and Ser^2 absent. Molecule B has 171 residues, with Met^1 absent. Gly^{171} and Ser^{172}, adducts of cloning, were clearly visible in the electron density maps of both molecules. The Arg^{22} and Glu^{100} side chains in molecule A were incomplete because of poor electron densities, and in molecule B the Ser^2, Gln^3, Arg^{21}, Arg^{22}, Glu^{83}, and Glu^{112} side chains were incomplete for the same reason.

The following side chains were modeled in alternative conformations, Molecule A, Thr^{6}, Glu^{24}, Glu^{25}, Thr^{28}, Gln^{38}, Glu^{83}, Arg^{97}, Ser^{110}, Glu^{113}, Thr^{118}, and Ile^{133} and molecule B, Thr^{6}, Thr^{28}, Leu^{92}, Arg^{97}, Glu^{100}, Se-Met^{108}, Thr^{118}, Ile^{133}, and Arg^{160}. Phe^{134} in the hydrophobic core of the molecule was replaced by leucine, probably as a mutation introduced by a polymerase chain reaction. Seven sulfate ions, three acetate molecules, and 238 water molecules were also revealed in the model. Four of the sulfates are bound to molecule A and three to molecule B.

The MoaB monomer is ~32 × 35 × 50 $Å^3$ and consists of a six-strand β sheet, six α helices, and one 3_{10} helix packed in a modified Rossman fold (Fig 2*A*). The twisted β sheet with a $\beta_2 \uparrow \beta_1 1 \uparrow \beta_3 \uparrow \beta_6 \uparrow \beta_5 \downarrow \beta_4 \uparrow$ topology is formed by five parallel β strands, β_2 (residues 43–50), β_1 (12–18), β_3 (72–76), β_6 (131–136), β_4 (97–98), and one antiparallel β_5 (124–128) inserted between β_6 and a very short β_4. The β sheet is sandwiched between four α helices, a_1 (residues 23–40) and α_5 (139–150) on one side and α_2 (53–67) and α_3 (86–92) on the other. The three remaining helices are α_4 (99–115), a one-turn α_6 (164–168), and a 3_{10} helix (116–121). Helices α_1 and α_5 are distorted to various degrees.

Each of the molecules in the asymmetric unit is incorporated in a compact trimer generated by the 3-fold crystallographic axis. In this formation, each monomer interacts with two other monomers (Fig. 2*A*). The buried surface area within each pair of monomers in the trimer is ~1700 $Å^2$, whereas the total surface area of a monomer is ~8400 $Å^2$. The major contributor to trimer stability is the insertion of the 3_{10} helix of one monomer into the hydrophobic groove of another, which is formed between helices α_4, α_5, and the loop connecting α_5 and α_6. There is also a network of hydrogen bonds and salt bridges between each pair of monomers (Table III).

Two trimers form a hexamer, mostly through hydrophobic interactions at their interface. Size-exclusion chromatography showed that MoaB is a hexamer in solution as well (Fig. 3). In crystals, hexamerization buries a total of 2680 $Å^2$ (32%) of the surface of each monomer. Strong interactions in the observed hexamer, together with the conservation of some residues involved in its formation (Table III), lead us to believe that the oligomeric state of MoaB in crystals is the same as in solution and is biologically relevant.

The shape of the hexamer can be roughly described as an ~62-Å-high cylinder with a radius of ~35 Å. It has an equatorial groove formed between the trimers and three vertical clefts each formed by four molecules of the hexamer (Fig. 2*B*). The vertical clefts of the hexamer are lined with polar and mostly positively charged residues. The sides of the hexamer between each pair of vertical clefts are mostly neutral but with some negatively charged and a considerable number of hydrophobic residues. Three holes, ~8 × 11 Å, on the sides of the hexamer lead to a large cave inside of it. The bases of the cylinder are rather flat, formed by three pairs of helices α_1 and α_5 from each monomer of the trimer. Judging by the area of buried surface and the number and character of interactions, the trimer appears to be a more stable formation than the hexamer.

Analysis of Structural Similarities and the Putative Active Site

A structural similarity search using the DALI algorithm (37) indicated that MoaB shares a common fold with several proteins also involved in Moco synthesis. MoaB had highly significant similarity with the G domains of the multifunctional mammalian protein gephyrin (12, 38), the plant protein Cnx1 (38), with *E. coli* MogA (19), and with the largest domain of MoeA (21, 22). Z-scores were 22.0, 21.9, 19.5, and 10.9, respectively. The corresponding root mean square deviations with these homologous structures were 1.38 Å for the 150 aligned C^{α} atoms, 1.47 Å for 147 C^{α} atoms, 1.73 Å for 147 C^{α} atoms, and 1.88 Å for 126 C^{α} atoms.

In addition to the structural conservation of several proteins along the Moco pathway, oligomerization of these proteins is also remarkably well preserved (Fig. 4). Thus, the functional trimer of MogA (19) is also seen in gephyrin and Cnx1 oligomers, although the latter two are multidomain proteins. The MoaB hexamer comprises two such trimers (Fig. 4*C*).

The extent of structural similarity between MoaB and the gephyrin and Cnx1 proteins is not reflected in amino acid sequence similarity. The sequence identities of MoaB with the G domains of Cnx1 and gephyrin, with MogA, and with the largest domain of MoeA are 33, 32, 27, and 21.5%, respectively. The structural similarity between MoaB and two other proteins from the Moco synthesis pathway, MoaC and MobA, is significantly lower, with respective root mean square deviations of 3.22 Å for 57 C^{α} atoms and 3.38 Å for 72 C^{α} atoms.

A number of residues are highly conserved among MoaB orthologs. Asp^{27}, Gly^{30}, Asp^{85}, Glu^{89}, Gly^{126}, Gly^{138}, Ser^{139}, and the motif Gly^{77}-Gly^{78}-Thr^{79}-Gly^{80} are invariant in MoaB proteins from 22 genomes. Pro^{137}, which is conserved in all but two of these sequences forms another conserved motif Pro^{137}-Gly^{138}-Ser^{139}. Sixteen other residues are similar, indicating conservation of mostly hydrophobic and a few polar interactions. These residues are Ile/Leu/Val15, Leu/Ile/Val16, Ala/Thr87, Leu/Ile/Val94, Phe/Leu/Ile95, Arg/Lys97, Phe/Ile102, Phe/Ile106, Arg/His107, Ser/Thr121, Arg/Lys-122, residues 132–134, Met/Leu136, and Ile/Leu/Val150.

When the MoaB sequence is aligned with the sequences of four other Moco synthesis proteins (referred to here as the Moco synthesis group), *E. coli* MogA, mammalian gephyrin, insect cinnamon, and plant Cnx1, 19 residues are invariant and a number of others show strong conservation (Fig. 5). Most of the invariant residues in the MoaB orthologs and the Moco synthesis group overlap, and only a few belong to either group exclusively. For example, the amino acids in positions (according to the MoaB sequence) 57, 90, 98, and 119 are invariant only in the Moco synthesis group, whereas the residues Gly^{30}, Gly^{126}, and Ser^{139} are highly conserved in MoaB orthologs only.

All of the invariant residues throughout the MoaB orthologs and the Moco synthesis group are in or near the depression on the surface of MoaB between two monomers of the MoaB trimer (Fig. 2*B*) where two of the bound sulfates are found (Figs. 2*B* and 6). A very similar depression is found in the MogA, gephyrin, and Cnx1 structures.

The polypeptide segments in the area of the MoaB surface depression are structurally the most preserved. These segments are formed by two motifs, Gly^{77}-Gly^{78}-Thr^{79}-Gly^{80} and Pro^{137}-Gly^{138}-Ser^{139}. In both the MoaB and MogA structures, these motifs are responsible for binding one of the sulfates (Fig. 6*B*). The Ser^{121} side chain, using the MoaB nomenclature, also contributes to binding. This residue is Ser or Thr in all MoaB orthologs conserving the interacting hydroxyl group.

It is likely that these structurally conserved sites are occupied by phosphate groups of physiological compounds, a conjecture that is supported by the electron density map. As can be seen on Fig. 7, the electron density in this region cannot be entirely accounted for by Pho1. Remarkably, a very similar feature can be found in the structure of MogA. It has been suggested (19) that this could be a remnant of some phosphate-containing compound that was bound to the protein strongly enough so as not to be completely dissociated during purification and crystallization. Another sulfate in our structure is bound to a much less conserved region of the same depression (see Figs. 6 and 7). This region is generally quite flexible as indicated by high *B* factors. Part of this binding site is missing in the MogA model due to disorder as is the second bound ion. Two more sulfate ions in molecule A and

one in molecule B are bound at the C terminus. It is difficult to assess the physiological importance of these ions, because two of the residues at this end are adducts of cloning.

Labeled GTP Binding in Solution

Our modeling studies indicate that GTP may bind in the putative active site of MoaB. To establish reaction conditions for potential GTP binding by the MoaB protein, pH was modulated from 5.0 to 8.0, and [α-^{32}P]GTP binding was monitored by protein precipitation followed by scintillation counting. GTP binding was most efficient at pH 7.5; therefore, reactions were performed at pH 7.5. Between 5 and 20% of input radioactivity was recovered, compared with less than 1% in mock reactions containing no protein, indicating the binding of GTP. Various divalent cations were added to determine their effect on MoaB GTP binding. The results showed that Mg^{2+} had no impact on binding, Ca^{2+} was inhibitory, and Mn^{2+} was stimulatory (Fig. 8*A*). GTPase activity was assessed by monitoring reaction products with thin-layer chromatography (Fig. 8*B*). Ca^{2+} again appeared to decrease overall activity, whereas Mn^{2+} acted both to increase overall binding and to modulate the ratio of GDP to GTP bound to the MoaB protein. In the presence of all three cations (Mg^{2+}, Ca^{2+}, and Mn^{2+}) simultaneously, the stimulatory and modulatory effects of Mn^{2+} were abated.

DISCUSSION

The exact role of MoaB in Moco biosynthesis is unknown. Strong structural similarity of MoaB to MogA and to G domains of mammalian gephyrin and plant Cnx1 (Fig. 4), which are also involved in the Moco biosynthesis, together with the sequence (Fig. 5) and spatial (Fig. 6) conservation of several residues, suggests a conserved function among these proteins. Although the bound molybdopterin has not been observed crystallographically, MogA, mammalian gephyrin, and plant Cnx1 bind to it with high affinity (12, 19, 39). The high degree of sequence and structural conservation in the surface depression suggests that this cavity may be a consensus binding site for molybdopterin.

Liu *et al.* (19) mutated several highly conserved residues in MogA to Ala to study their possible role in function. The MogA residues studied were Ser^{12}, Asp^{49}, Thr^{76}, Arg^{81}, Asp^{82}, Ser^{107}, and Ser^{117}; the corresponding residues in MoaB are Ser^{19}, Glu^{52}, Thr^{79}, Arg^{84}, Asp^{85}, Ser^{110}, and Ser^{121}, many of which are also well conserved (Figs. 4–6). The only mutations that had a measurable effect on MogA activity were D49A and D82A. They were assumed to disrupt catalysis, because molybdopterin binding in the two mutant proteins was shown to be improved (19). The corresponding residues in MoaB, Glu^{52} and Asp^{85}, are highly conserved both in primary and in tertiary structures and could play a similar role. In MogA, the proposed catalytic site contained electron density that was modeled as a sulfate ion but was proposed to correspond to the remnants of molybdopterin (19). In the MoaB structure, we observed very similar electron density (Fig. 7). Thus, the overall conservation of the binding site and of the interaction with the bound anion suggests that MoaB might bind MTP similarly to MogA, gephyrin, and Cnx1.

The two presumed phosphate ions in MoaB could be consistent with a binding of GTP, which was easily modeled in the putative binding site of MoaB (Fig. 7). In this model, the α and γ phosphate groups of GTP are very close to the positions of the ions bound in the crystal structure. The putative catalytic Asp^{85} and Glu^{52} interact directly with these phosphates and are ideally poised to play a role, perhaps in the transformation of GTP into precursor Z. The base of the modeled GTP fits very well in the deep cavity, which is occupied by several water molecules in our crystal structure. The invariant Ser^{110} (Figs. 5 and 6) is located in a deep cleft where the base of the modeled GTP is bound (Fig. 7) and could interact with the N-1 and/or N-2 atoms of the latter. Our results show that MoaB indeed binds GTP (Fig. 8*A*), but with low affinity. The protein also possessed a low GTPase

activity (Fig. 8*B*). Both binding and enzymatic potential were affected by some divalent ions, especially by Mn^{2+}. Coincidentally, when some divalent ions were added in crystallization trials of another Moco synthesis protein, MoeA, Mn^{2+} appeared to have more drastic effects than the others.[2]

Based on the possibility of binding various compounds of Moco pathway by MoaB and on its structural similarity with MogA and MoeA, we suggest that MoaB might play a substrate-shuttling role in the biosynthetic process. The intermediates of Moco synthesis and the cofactor are unstable, suggesting that the reactions, including the transfer of Moco to apomolybdoenzymes, occur while the corresponding compounds are still bound to the enzymes or to transporter/storage proteins, avoiding their dissociation into the external solvent.

The protection of the substrates against solvent might occur through specific protein-protein interactions among the enzymes. It is becoming apparent that protein-protein interactions play crucial role in Moco biosynthesis. Magalon *et al.* (40) reported that numerous protein pairs from the Moco pathway do form complexes *in vivo*, including MobB-MoeA, MobB-MogA, MoeA-MogA, MoeA-MobA, and MobB-MobA and that some compounds of this pathway influence these interactions. Divalent ions, as shown here, can also influence binding of some compounds in the Moco pathway, although the mechanism of such influence is not yet clear.

Possible involvement of MoaB in such protein-protein interactions is supported indirectly by several observations. First, in *Synechococcus sp.*, the MoaC ortholog is fused to the homolog of either MoaB or MogA (41). Second, MogA and MoeA are combined to form the multifunctional protein gephyrin in mammals (13), Cnx1 in plants (15), and cinnamon in insects (14). All of the protein-protein complexes observed *in vivo* (40, except for MobB-MobA, contain either MogA or MoeA, the structural homologs of MoaB. If MoaB can indeed bind GTP, precursor Z, or molybdopterin as discussed above and if it can form complexes with several other proteins of Moco synthesis pathway, it is tempting to suggest that MoaB plays a transporting and/or storage role.

The presence of six independent binding sites in the MoaB hexamer would enhance the capacity of the protein in such a role. As reported by Schwarz *et al.* (39), the G domain of Cnx1 can be present in both hexameric and trimeric forms. Because the trimer of Cnx1 G domain is very similar to the trimer of MoaB, and because the trimer of MoaB seems to be much more stable than its hexamer, it is possible that MoaB is also present in these two states of oligomerization. In our experiments with size-exclusion chromatography, MoaB was not found in a trimeric state. However, equilibrium between trimeric and hexameric states could be modulated by particular compounds, such as reaction substrates and products, ions, or other proteins of the pathway, all of which were absent in our experiments. In the trimeric state MoaB could bind MobB and MoeA much the same way as does MogA (40). On the other hand, MogA could replace one-half of the MoaB hexamer, as shown on Fig. 4*C*. The largest structural differences between MoaB and MogA are at the bases of the MoaB hexamer, away from the trimer-trimer interface. Formation of such heterooligomers could be an effective way of substrate/product exchange along the Moco pathway without their dissociation into the external solvent. An inferred promiscuity of MoaB in protein-protein complex formation would be an asset for a transporter/storage protein.

[2]R. Sanishvili, unpublished results.

Summary

The crystal structure of *E. coli* MoaB was determined at 1.6-Å resolution. The strong structural similarity of MoaB with other Moco synthesis proteins, such as MogA, gephyrin, and Cnx1, along with the amino acid conservation patterns, indicated that MoaB might bind some of the same compounds, namely molybdopterin. The presence of a sulfate ion in the putative binding site, the experimental verification of MoaB/GTP binding, and modeling studies suggest that GTP and possibly precursor Z could bind in the same binding site.

MoaB displayed very strong structural similarity to MogA and MoeA, two proteins that form numerous complexes with other proteins within the Moco synthesis pathway in *E. coli*, suggesting that MoaB might be part of such complexes and may play a role in transport or storage of several compounds in the Moco synthesis pathway.

REFERENCES

1. Hille R. Essays Biochem. 1999; 34:125–137. [PubMed: 10730192]
2. Romao MJ, Knablein J, Huber R, Moura JJ. Prog. Biophys. Mol. Biol. 1997; 68:121–144. [PubMed: 9652170]
3. Rajagopalan KV, Johnson JL. J. Biol. Chem. 1992; 267:10199–10202. [PubMed: 1587808]
4. Rajagopalan KV. Biochem. Soc. Trans. 1997; 25:757–761. [PubMed: 9388540]
5. Rajagopalan KV. Adv. Enzymol Relat. Areas Mol. Biol. 1991; 64:215–290. [PubMed: 2053467]
6. Rothery RA, Blasco F, Magalon A, Weiner JH. J. Mol. Microbiol. Biotechnol. 2001; 3:273–283. [PubMed: 11321583]
7. Boyington JC, Gladyshev VN, Khangulov SV, Stadtman TC, Sun PD. Science. 1997; 275:1305–1308. [PubMed: 9036855]
8. Rajagopalan, KV. Escherichia coli and Salmonella. Neidhardt, FC., editor. ASM Press; Washington D.C.: 1996. p. 674-679.
9. Palmer T, Vasishta A, Whitty PW, Boxer DH. Eur. J. Biochem. 1994; 222:687–692. [PubMed: 8020507]
10. Stevenson CE, Sargent F, Buchanan G, Palmer T, Lawson DM. Structure Fold. Des. 2000; 8:1115–1125. [PubMed: 11080634]
11. Lake MW, Temple CA, Rajagopalan KV, Schindelin H. J. Biol. Chem. 2000; 275:40211–40217. [PubMed: 10978347]
12. Sola M, Kneussel M, Heck IS, Betz H, Weissenhorn W. J. Biol. Chem. 2001; 276:25294–25301. [PubMed: 11325967]
13. Ramming M, Kins S, Werner N, Hermann A, Betz H, Kirsch J. Proc. Natl. Acad. Sci. U. S. A. 2000; 97:10266–10271. [PubMed: 10963686]
14. Kamdar KP, Primus JP, Shelton ME, Archangeli LL, Wittle AE, Finnerty V. Biochem. Soc. Trans. 1997; 25:778–783. [PubMed: 9388544]
15. Stallmeyer B, Nerlich A, Schiemann J, Brinkmann H, Mendel RR. Plant J. 1995; 8:751–762. [PubMed: 8528286]
16. Kozmin SG, Pavlov YI, Dunn RL, Schaaper RM. J. Bacteriol. 2000; 182:3361–3367. [PubMed: 10852865]
17. Wuebbens MM, Liu MT, Rajagopalan K, Schindelin H. Structure Fold. Des. 2000; 8:709–718. [PubMed: 10903949]
18. Reiss J. Hum. Genet. 2000; 106:157–163. [PubMed: 10746556]
19. Liu MT, Wuebbens MM, Rajagopalan KV, Schindelin H. J. Biol. Chem. 2000; 275:1814–1822. [PubMed: 10636880]
20. McLuskey K, Harrison JA, Schuettelkopf AW, Boxer DH, Hunter WN. J. Biol. Chem. 2003; 278:23706–23713. [PubMed: 12682065]
21. Xiang S, Nichols J, Rajagopalan KV, Schindelin H. Structure (Lond.). 2001; 9:299–310.

22. Schrag JD, Huang W, Sivaraman J, Smith C, Plamondon J, Larocque R, Matte A, Cygler M. J. Mol. Biol. 2001; 310:419–431. [PubMed: 11428898]
23. Rudolph MJ, Wuebbens MM, Rajagopalan KV, Schindelin H. Nat. Struct. Biol. 2001; 8:42–46. [PubMed: 11135669]
24. Altschul SF, Madden TL, Schaffer AA, Zhang J, Zhang Z, Miller W, Lipman DJ. Nucleic Acids Res. 1997; 25:3389–3402. [PubMed: 9254694]
25. Zhang RG, Skarina T, Katz JE, Beasley S, Khachatryan A, Vyas S, Arrowsmith CH, Clarke S, Edwards A, Joachimiak A, Savchenko A. Structure (Lond.). 2001; 9:1095–1106.
26. Matthews BW. J. Mol. Biol. 1968; 33:491–497. [PubMed: 5700707]
27. Evans G, Pettifer RF. J. Appl. Crystallogr. 2001; 34:8286.
28. Westbrook EM, Naday I. Methods Enzymol. 1997; 276:244–268. [PubMed: 9048377]
29. Pflugrath JW. Acta Crystallogr. D. Biol. Crystallogr. 1999; 55:1718–1725. [PubMed: 10531521]
30. Otwinowski Z, Minor W. Methods Enzymol. 1997; 276:307–326.
31. Scheffers DJ, Driessen AJ. Mol. Microbiol. 2002; 43:1517–1521. [PubMed: 11952901]
32. Brunger AT, Adams PD, Clore GM, DeLano WL, Gros P, Grosse-Kunstleve RW, Jiang JS, Kuszewski J, Nilges M, Pannu NS, Read RJ, Rice LM, Simonson T, Warren GL. Acta Crystallogr. D. Biol. Crystallogr. 1998; 54:905–921. [PubMed: 9757107]
33. Perrakis A, Morris R, Lamzin VS. Nat. Struct. Biol. 1999; 6:458–463. [PubMed: 10331874]
34. Murshudov GN, Vagin AA, Dodson EJ. Acta Crystallogr. D. Biol. Crystallogr. 1997; 53:240–255. [PubMed: 15299926]
35. Jones TA, Zou JY, Cowan SW, Kjeldgaard M. Acta Crystallogr. Sect. A. 1991; 47:110–119. [PubMed: 2025413]
36. Berman HM, Westbrook J, Feng Z, Gilliland G, Bhat TN, Weissig H, Shindyalov IN, Bourne PE. Nucleic Acids Res. 2000; 28:235–242. [PubMed: 10592235]
37. Holm L, Sander C. Proteins. 1994; 19:165–173. [PubMed: 7937731]
38. Schwarz G, Schrader N, Mendel RR, Hecht HJ, Schindelin H. J. Mol. Biol. 2001; 312:405–418. [PubMed: 11554796]
39. Schwarz G, Boxer DH, Mendel RR. J. Biol. Chem. 1997; 272:26811–26814. [PubMed: 9341109]
40. Magalon A, Frixon C, Pommier J, Giordano G, Blasco F. J. Biol. Chem. 2002; 277:48199–48204. [PubMed: 12372836]
41. Rubio LM, Flores E, Herrero A. J. Bacteriol. 1998; 180:1200–1206. [PubMed: 9495759]
42. Nicholls A, Sharp KA, Honig B. Proteins. 1991; 11:281–296. [PubMed: 1758883]
43. Pitterle DM, Rajagopalan KV. J. Biol. Chem. 1993; 268:13499–13505. [PubMed: 8514782]
44. Leimkuhler S, Rajagopalan KV. J. Biol. Chem. 2001; 4:4.
45. Thompson JD, Higgins DG, Gibson TJ. Nucleic Acids Res. 1994; 22:4673–4680. [PubMed: 7984417]

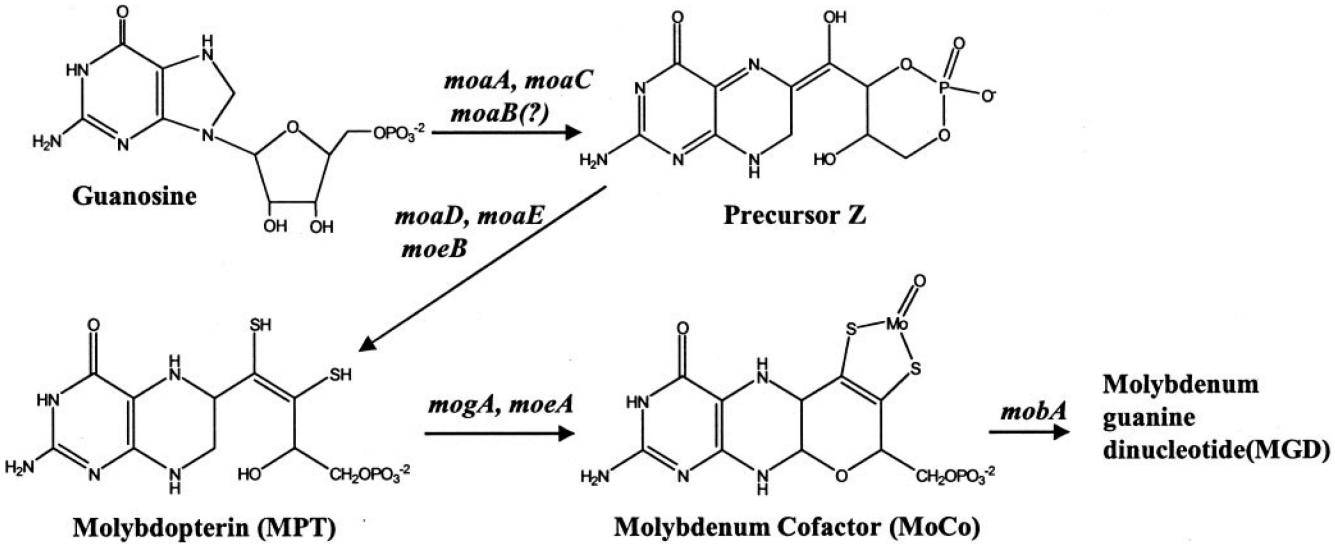

Fig. 1. Moco biosynthesis pathway in *E. coli*

The four-step synthesis first involves the conversion of a guanosine derivative to an unstable intermediate, precursor Z, through the action of the enzymes MoaC and MoaA. The heterotetrameric enzyme molybdopterin synthase ($MoaD_2$: $MoaE_2$) then incorporates sulfur from the C-terminal thiocarboxylate of MoaE onto precursor Z to form the dithiolene group of molybdopterin (23, 43, 44). The incorporation of molybdenum into molybdopterin to form Moco requires the proteins MogA and MoeA (19). On the last step, a GMP group is transferred to the terminal phosphate of Moco by the product of the gene *mobA* (9–11) to form MGD.

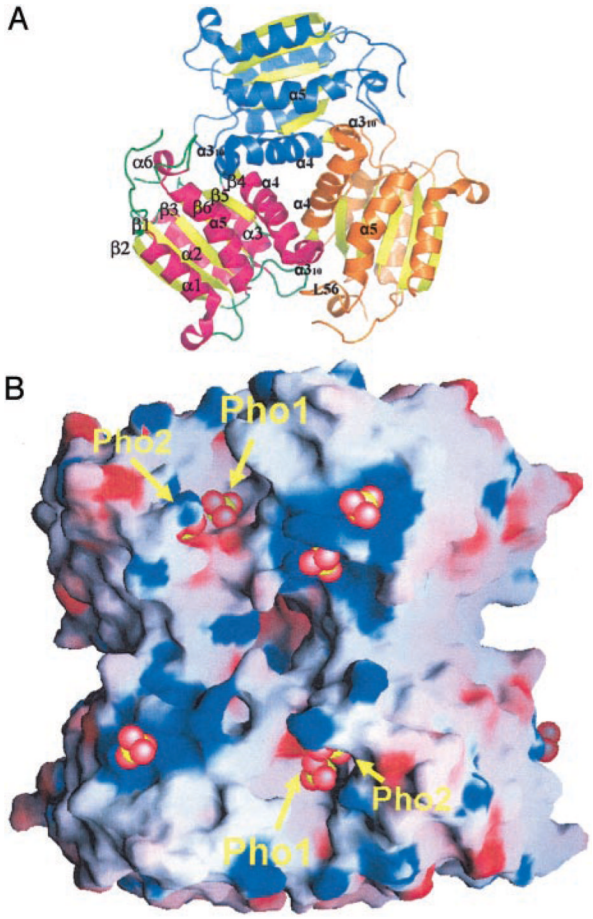

Fig. 2. Oligomerization of MoaB

A, view of a trimer along the crystallographic 3-fold axis. Six strands of the β sheet (*yellow*), along with α and 3_{10} helices (*pink*), are labeled in one monomer. The 3_{10} helix (perpendicular to the plane of the paper) of one monomer forms rich hydrophobic interactions in the cleft created by helices α4, α5, and the loop between α5 and α6 (labeled *L56*) of the other. *B*, electrostatic representation of the surface of MoaB hexamer. *Red* and *blue* correspond to the negatively and positively charged areas, respectively, whereas *white* represents neutral regions. The hexamer can be approximated as a cylinder 62-Å high with a radius of 35 Å. Longitudinal and equatorial grooves are also visible intersecting at the central hole created between the four monomers. Bound sulfate ions are represented with *red* (oxygens) and *yellow* (sulfur) spheres. Two sulfate ions, which could mimic the phosphate groups in the binding site, are labeled *Pho1* and *Pho2*. The binding of remaining sulfates is probably opportunistic. Fig. 2*B* was prepared with GRASP (42).

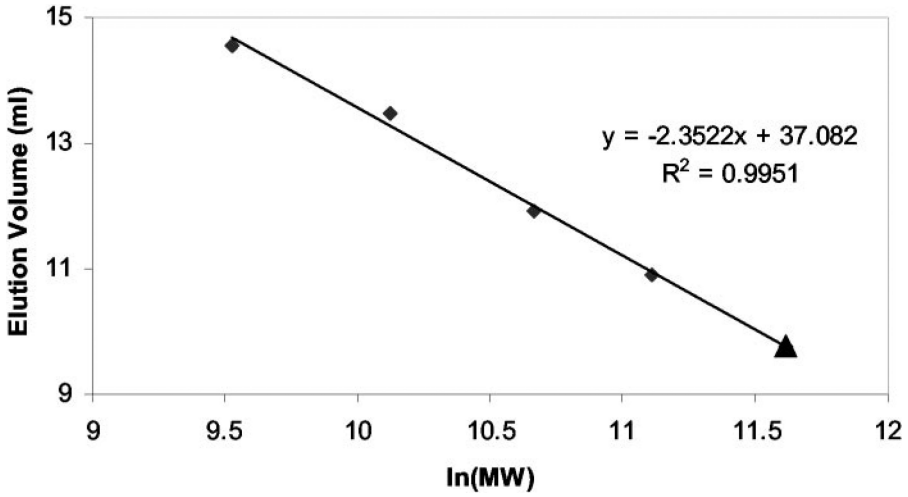

Fig. 3. Size-exclusion chromatography of *E. coli* MoaB

Size-exclusion fast protein liquid chromatography was performed using a Superdex-75 column (Amersham Biosciences). The purified MoaB protein (▲) eluted from the column with an apparent molecular mass of ~111.2 kDa. Standard markers (◆), albumin (67 kDa), ovalbumin (43 kDa), chymotrypsinogen A (25 kDa), and ribonuclease A (13.7 kDa) (Amersham Biosciences), were used to calibrate the column. The best-fit line is shown with the R^2 value of the fit indicated.

Fig. 4. Structural similarity of MoaB with MogA and gephyrin

A, superposition of the MoaB (*orange*) and MogA (*marine*) monomers shows very good alignment of secondary structure elements and many of the loops. The only significant difference is caused by two insertions in the MogA amino acid sequence, corresponding to the protruding β turn (labeled *1*) and β hairpin (labeled *2*). *B*, superposition of C^{α} traces of MoaB (*pink*) and gephyrin G domain (*green*) trimers. The latter is more similar to MoaB than MogA, because it does not have protrusions, which are characteristic for MogA and shown in *A*. *C*, the MoaB hexamer is shown with a *pink* semitransparent surface. A wire model of the MogA trimer fits in half of the hexamer very well, except for the protrusions shown in *A*.

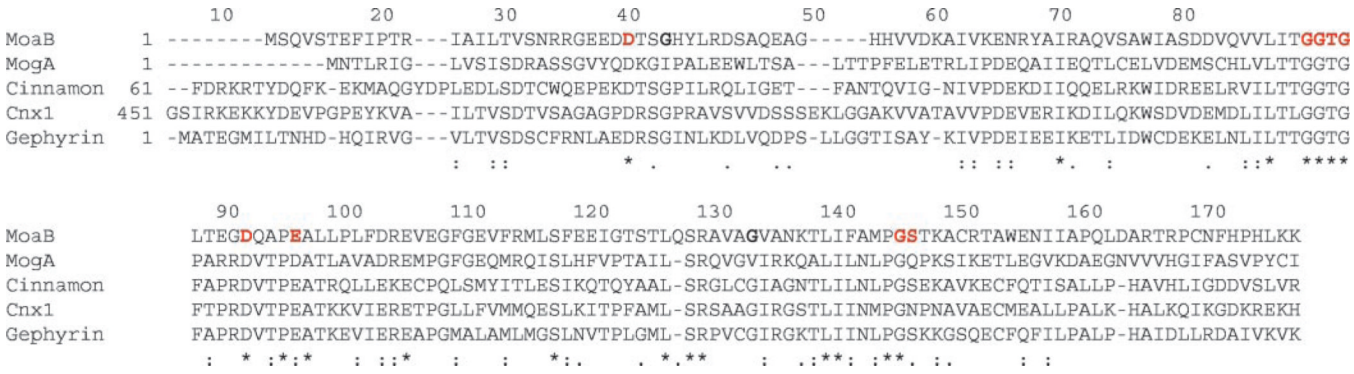

Fig. 5. Sequence alignment of *E. coli* MoaB, MogA, *Drosophila* cinnamon, *Arabidopsis* Cnx1, and human gephyrin performed with ClustalW (45)

For the last three proteins, only portions homologous to MoaB and MogA are presented. *Numbers* after the protein names indicate the starting amino acid number of a given sequence. *asterisk*, depicts invariant residues; *colon*, corresponds to conservation of a residue type (*e.g.* hydrophobic, positively charged, carrying hydroxyl group); *dot*, indicates that only one residue interrupts an otherwise conserved type. Residues invariant in 22 MoaB orthologs are shown in *bold red*. Pro^{137}, although not identified here as invariant in MoaB orthologs, changes to Ala in only 2 of 22 sequences.

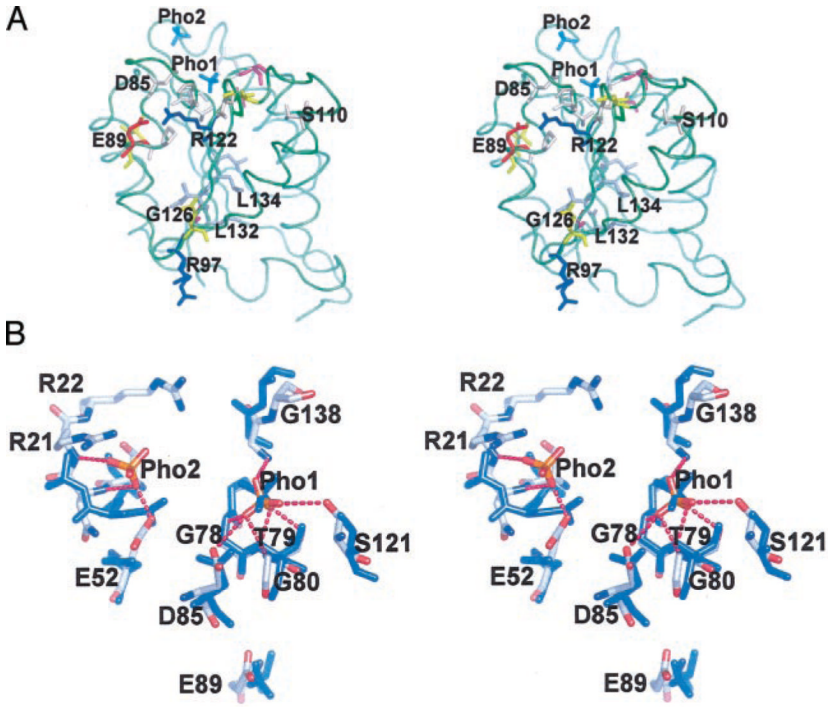

Fig. 6. Conserved residues and the binding site of MoaB

A, the overall fold of MoaB is shown in *green* with two sulfate ions in *cyan. Light beige* residues are conserved in all 22 orthologs as well as in the other Moco proteins listed (not labeled). *Blue* residues (Arg^{97} and Arg^{122} in MoaB) vary only to lysine, thus conserving a positive charge. Glu^{89}, which is invariant in MoaB orthologs, is aspartic acid in other Moco proteins. *Gray* represents the residues conserving the hydrophobicity in MoaB orthologs and in other four Moco proteins. Three residues shown in *magenta*, Glu^{30}, Gly^{125}, and Ser^{139}, are invariant in the 22 MoaB sequences but not in gephyrin, MogA, Cnx1, or cinnamon. Conversely, the *yellow* residues in positions 57, 90, 98, and 137 (MoaB nomenclature) are invariant in the latter group but vary in MoaB sequences. The Arg^{97} and Ser^{110} side chains are shown in two alternative conformations. *B*, ion binding details in MoaB and MogA. The MoaB residues, interacting with bound sulfates are shown with *gray* carbons, *blue* nitrogens, and *red* oxygens. Corresponding residues from MogA are *light blue*. The region around Pho2 is flexible with higher *B* factors. Although it is shown in full, only parts of the Arg^{22} side chain could be modeled because of its disorder. This segment is more disordered and is missing in MogA structure (19). Both sulfate groups are primarily bound by their interactions (*magenta dashed lines*) with the backbone nitrogens. Motif Gly^{77}-Gly^{78}-Thr^{79}-Gly^{80}, a major contributor to Pho1 binding, is particularly well conserved structurally. The putative catalytic Asp^{85} also interacts with this Pho1.

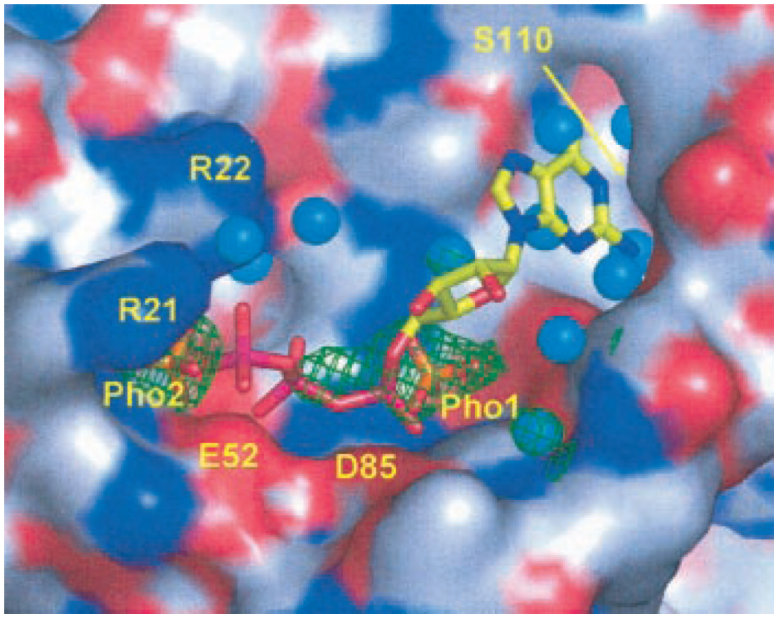

Fig. 7. Modeled GTP in the binding site of MoaB

The surface of the protein containing the binding site is color-coded with *red* oxygens, *blue* nitrogens, and *gray* carbons. Experimentally observed sulfate ions (*orange* S and *red* O atoms) are shown with their corresponding $2F_o - F_c$ electron densities contoured at a 1σ level (*green mesh*). Water molecules are shown as *cyan spheres*. Sulfates are labeled Pho1 and Pho2 because they likely are phosphate groups *in vivo*. Associated with Pho1, electron density has an additional feature, which cannot be explained with the sulfate ion and which extends toward Pho2. It is likely the remnant of a phosphate-containing compound from the physiological complex. Arg^{21} and Arg^{22} are also labeled. The guanidinium group of the Arg^{22} side chain is not entirely visible in our structure but is added in this figure to show its proximal position and to avoid the creation of an apparent extended surface depression that could lead to erroneous interpretations. The ridge, separating two deeper cavities on either side of Pho1, is formed by two conserved motifs, Gly^{77}-Gly^{78}-Thr^{79}-Gly^{80} and Pro^{137}-Gly^{138}-Ser^{139}. Modeled GTP is shown with *stick* model color coded as *yellow* carbons, *blue* nitrogens, *red* oxygens, and *magenta* phosphors. The locations of the Glu^{52} and Asp^{85} carboxyl groups are indicated with *labels*, and the location of Ser^{110} is shown with an *arrow*.

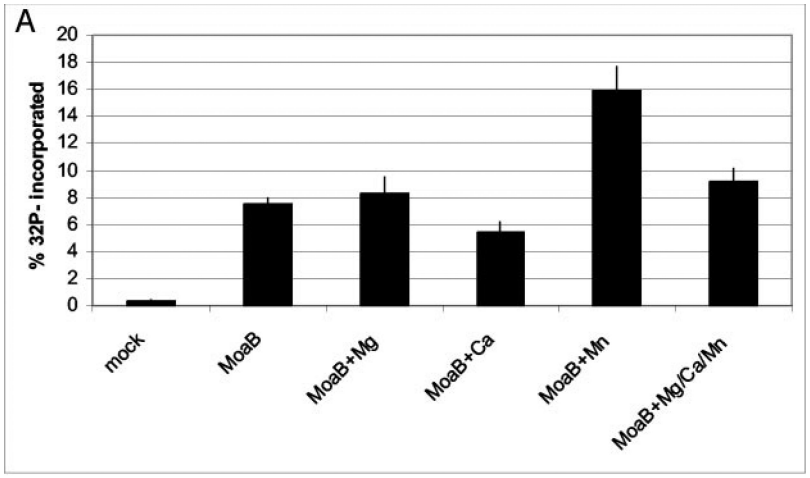

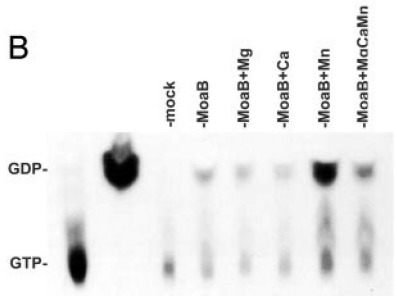

Fig. 8. GTP binding and GTPase activity in MoaB

A, incorporation of radio-labeled GTP. Binding reactions were assembled using [α-^{32}P]GTP as a tracer and either no protein (*mock*), MoaB protein alone (*MoaB*), or MoaB protein with the listed divalent cations (+*Mg/Ca/Mn*). Protein precipitations were performed as described under "Experimental Procedures." The amount of bound [α-^{32}P]GTP was determined by scintillation counting and is expressed as a percentage of the total input [α-^{32}P]GTP. *B*, GTPase activity. Binding reactions were assembled as in *A*. Protein was precipitated, acid-hydrolyzed, and analyzed by thin-layer chromatography as described under "Experimental Procedures." Input [α-^{32}P]GTP (*lane 1*) and enzymatically derived [α-^{32}P]GDP (*lane 2*) were used as running standards.

Table I

Basic data collection and processing statistics for MoaB crystals

The number of amino acid residues/methionines (including N-terminal Met) was 340/6. The number of molecules in the asymmetric unit was 2. The R_{merge} between low- and high-resolution passes was 0.037. Crystal lattice P321 $a = b = 69.11$, $c = 126.22$ Å $\alpha = \beta = 90°$ $\gamma = 120°$.

	Inflection point	Peak	Low resolution	High resolution
Energy (keV)	12.65934	12.66075	12.000	12.000
Wavelength (Å)	0.97954	0.97929	1.03321	1.03321
Resolution (Å)	50–1.87	50–1.87	50–2.7	3.0–1.54
No. of observations	311,387	311,440	60,562	251,553
Unique[a] reflections	55,534	55,494	8,840	45,003
Completeness (%)[b]	99.4 (99.0)	99.2 (98.0)	86.8 (90.2)	99.5 (95.8)
I/σ(I)[b]	26.5 (2.5)	26.2 (2.3)	28.9 (14.5)	22.4 (2.6)
R_{sym}[b]	0.057 (0.45)	0.06 (0.52)	0.056 (0.137)	0.067 (0.41)

[a] Bijvoet pairs for scaling the multiwavelength anomalous dispersion data sets were kept separately.

[b] Statistics in the last resolution shell are in parentheses.

Table II

Phasing and refinement statistics for MoaB structure

Phasing in 50–2.5-Å resolution shell	Inflection point	Peak	FOM[a]
Number of reflections	17,750 (1754)	22,885 (2607)	23,021 (2641)
Phasing power with			
2 sites	2.44 (1.71)	2.42 (1.67)	0.60 (0.48)
2 sites + disorder	2.83 (1.93)	2.74 (1.85)	0.66 (0.54)
4 sites + disorder	2.95 (2.18)	2.90 (2.07)	0.67 (0.55)

Refinement		
Resolution (Å)	62–1.60	1.64–1.60
Number of reflections	42215	2867
R-factor %	18.5	20.6
R_{free} %	21.9	27.1
Correlation	96.2	
Correlation free	95.2	
All nonhydrogen atoms	2961	
Mean *B*-factor	14.77	

Deviations from ideal	Refined	Target
Covalent bonds	0.020	0.021
Bond angles	1.885	1.955
Planarity	0.007	0.02
Chiral centers	0.107	0.20
Torsion angles	6.285	5.0
van der Waals contacts	0.240	0.30

[a]Mean FOM after density modification in 50–2.0-Å shell was 0.92.

Table III
Polar interactions in the interface within the trimer

Some of the residues are highly conserved in MoaB sequences across 22 organisms. For example, Glu^{89} is invariant, whereas residues 97, 104, 107, and 122 have conserved charges.

Atom in monomer 1	Atom in monomer 2	Distance
		(Å)
O Glu^{83}	NH-2, Arg^{97}	3.17
OE-2 Glu^{89}	NH-2 Arg^{97}	3.29
OE-2 Glu^{89}	NZ Arg^{97}	2.78
OE-1 Glu^{89}	NH-1 Arg^{122}	3.30
NH-2 Arg^{107}	OE-2 Glu^{100}	3.32
NH-2 Arg^{107}	OE-2 Glu^{104}	2.98
NZ Arg^{107}	OE-1 Glu^{104}	2.62
OG Ser^{117}	N Cys^{162}	3.21
OG Ser^{117}	O Cys^{162}	2.65
OG-1 Thr^{116}	NE-2 Gln^{154}	2.89
NE-2 Gln^{120}	OE-1 Gln^{154}	2.85